



In situ measurements of SO₂, NO_x, NO_y, and O₃ in Beijing, China during August 2008

Yang Sun, Lili Wang, Yuesi Wang ^{*}, Liu Quan, Liu Zirui

State Key Laboratory of Atmospheric Boundary Layer Physics and Atmospheric Chemistry (LAPC), Institute of Atmospheric Physics, Chinese Academy of Sciences, Beijing 100029, China

ARTICLE INFO

Article history:

Received 19 March 2010

Received in revised form 23 August 2010

Accepted 8 November 2010

Available online 18 December 2010

Keywords:

SO₂

NO_x

NO_z

OPE

SPM

ABSTRACT

The measurement of SO₂, O₃, NO, NO₂, and NO_y mixing ratios was conducted from Jul 28, 2008 to Sep 2, 2008 at the Institute of Atmospheric Physics, Chinese Academy of Sciences (IAP, CAS) station, which is 2 km southwest to the Beijing National Stadium (Bird's Nest/Olympic Stadium). Photochemical pollution was detected during the measurement on Aug 2, 2008, and the maximum hourly average [O₃] reached 128 ppbv, caused by both the local photochemical reactions and regional transportation of pollutants. The NO_x Ozone Production Efficiency (OPE (NO_x)) values were 6.9 and 20.2 on Aug 2 and Aug 24, 2008 respectively, which were the two days with highest O₃ pollution. The OPE (NO_x) of 6.9 on Aug 2 was within a typical range in city area, and it implied that the high O₃ could be due to local sources. While OPE (NO_x) of 20.2 on Aug 24 was larger than the typical value in the region, but lower than that of the surrounding clean area during 2008 Beijing Olympics Closing Ceremony. It indicated that the pollution was because of regional transportation of pollutants. In addition, 60% of the extent of the Smog Production Model (SPM) data was less than 0.6 and the rest was slightly larger than 0.6, with maximum of 0.78. It indicated that the sensitivity of O₃ generated was volatile organic compounds (VOCs) control during the observation period. The SPM results also implied that O₃ product in high-O₃ day is a transition state from VOCs sensitivity to NO_x sensitivity. Lastly, the analysis of the wind direction and extent of SPM showed that the photochemical pollution of this region was mostly subject to the influence of southeastern air flow in the summer.

© 2010 Elsevier B.V. All rights reserved.

1. Introduction

During the past 15 years, Beijing, the capital city of China, was undergoing a rapid economic development. The number of automobiles had been increased from 0.82 million in 1994 to 3.5 million in 2008. With the industrial activities and the number of automobiles increasing simultaneously, the VOCs and NO_x (NO + NO₂) emission will significantly increase in this region. It is commonly known that the tropospheric ozone originates mostly from the photochemical reactions of VOCs and NO_x. NO_x plays the role of catalyst in the chain reactions for ozone production. In addition, NO_x is also one of the major terminators of free radicals (Raivonen et al., 2009; Peng et al., 2006; Carl et al., 2001; Chameides et al., 1988; Guangfeng and Jerome, 2004; Cassandra et al., 2006). The NO_x emitted from fossil fuel combustion has a lifetime of less than a day against oxidation to HNO₃ and peroxyacetyl nitrate (PAN). The sum of NO_x, HNO₃, PAN, and other minor NO_x oxidation products is known as the total reactive nitrogen NO_y (Cardelino and Chameides, 1990; Paul et al., 2008; Ariel et al., 2005; Zhang et al., 2008; Thomas et al., 2005). NO_y also plays an essential role in the aeronomy of the atmosphere. It is a major cause of tropospheric pollution, and stratospheric ozone loss. Significant effort has been devoted to develop

an accurate and comprehensive method to measure the total NO_y and its component species.

The covariance of O₃ and NO_y or NO_z = (NO_y - NO_x) = HNO₃ + HONO + PAN + other nitrogen oxides is used to estimate an apparent O₃ production efficiency. This ratio is sensitive to the differences between the loss rate of O₃ and NO_y. Out of all the air pollution causes, photochemical smog is the major one leading to air quality deterioration. It is a great challenge for the air quality administration of Beijing to develop an effective control strategy for the photochemical smog. The major objective of this study is to improve the understanding of NO_x-NO_z-O₃ chemistry in Beijing, which is important for the development of O₃ reduction strategies, and the covariance of NO_y and SO₂ in ambient air yields an estimate of the primary emission ratios for urban pollution sources.

In this research, we investigated the concentration of SO₂, O₃, NO, NO₂, and NO_y that was measured at the meteorological observation tower located in the northern part of Beijing from Jul 28 to Sep 2. This paper is organized in the following structure. Section 2 is the description of the instruments and measurements, including the part of photolytic conversion of NO₂. Section 3 is the analysis of the measured data, to study the characterizations of ozone and the NO_x, NO_z and NO_y pollutants and chemical processes that control the O₃ formation. Some photochemical indicator ratios were calculated and the extent of reaction in the SPM was estimated. The VOCs- or NO_x-sensitive regime to the formation of ozone was identified in this region. Section 4 summarizes our conclusions and recommendations for the future research.

* Corresponding author.

E-mail address: wys@mail.iap.ac.cn (Y. Wang).

2. Instrumentation

During the Olympics observation period, the SO₂, O₃, NO, NO₂, NO_y measuring instrument provided by IAP was installed in an observatory at 8 m level of a meteorological observation tower. The meteorological observation tower (39°58' 27.6°N, 116°22' 17.5"E) is located in the northern part of Beijing, in between of the North Third Ring Road and the North Fourth Ring Road. The north-south oriented Badaling Expressway is located 200 m to the east of the tower, and the east-west oriented BeiTucheng West road is located 80 m to the north of the tower. There are no direct industrial sources of atmospheric pollutants near this place.

Ozone was measured by using a commercial UV photometric analyzer (Thermo Environmental Instruments (TEI) Inc.; Model 49i) with detection limit of 0.5 ppbv and precision of 1 ppbv. For NO₂ the most widely used method transforms other nitrogen-containing compounds such as HNO₃, PAN, etc. even low temperature catalytic molybdenum converts to a considerable extent. In this research, NO was measured using ECO PHYSICS CLD86 and NO₂ was measured using photolytic conversion of NO₂ to NO followed by NO/O₃ chemiluminescence and UV differential optical absorption spectroscopy. The PLC 860 with a detection limit of 20 pptv and a precision of 30 pptv, which is a photolysis converter made by ECO PHYSICS was used. The PLC 860 enables the measurement of NO₂ at much lower concentration levels and it is far more selective than would be possible using other converters based on chemical, thermal, or catalytic technology (Mannschreck et al., 2004). The NO_y analyzer is based on Thermo's Model 42C NO-NO₂-NO_x trace level analyzer with a detection limit of 0.5 ppbv and a precision of 1 ppbv. The major difference is that we utilized an external molybdenum converter, which minimized the sample transport distances thereby allowing the analyzer to measure more compounds that cannot be measured by an internal converter. SO₂ was detected by a pulsed UV fluorescence analyzer (TEI; Model 43i).

The detection limit of this analyzer is 0.05 ppbv for 2 min integration with precision of about 0.20 ppbv. These analyzers were all calibrated before the observation by injecting a span gas mixture in scrubbed ambient air generated by a TEI model 111. A NIST traceable standard in a cylinder (Scott Specialty Gases) containing 51.4 ppmv NO, and 48.2 ppmv SO₂ was diluted using a dynamic calibrator (TEI; Model 146) and ozone analyzers were calibrated at regular time intervals with a transfer standard (TEI; Model 49CPS). An automatic meteorological observation tower called Milos520 (Vaisala, Finland) was located at the 8-m height level, and observes the temperature, relative humidity and the speed and direction of wind in the atmosphere at ground level.

3. Results and discussion

3.1. Overview of the time series

The data analysis was based on the hourly average mixing ratio of each pollutant. Fig. 1 shows the time series of SO₂, O₃, NO-NO₂ and NO_y-NO₂ mixing ratios during the 2008 observation period. During the entire observation, [SO₂] was remained at a low level from Jul 28 to Aug 3, and the light showers on the 29th and 31st produced some wet scavenging effects. From Aug 3 to Aug 8, [SO₂] was high and the basic value was also relatively high. During this period, the weather status was stable. The wind direction remained as southwest; the wind speed was 1–3 m/s, and the temperature was quite high. All these conditions favored the slow spreading and accumulation of the pollutants, which were emitted from the southwest industrial zone.

Since Aug 8, [SO₂] started to decrease, which was probably because of the stricter source emission constrain due to the Olympic Games. Several heavily polluting factories were ordered to reduce their operating capacities or to completely shut down during the Games. All construction activities were placed on hold (Wang et al., 2009). It was

also associated with the changes in weather conditions (prolonged rainfall, decreased temperature, and more frequent air masses from clean regions) (Wang et al., 2010). The continuous shower and strong north wind on Aug 10 caused the [SO₂] dropped to the minimum level on this day, and after that, on Aug 13–15, 17, and 21, there were also intermittent rains, and the [SO₂] remained at a relatively low level. From Aug 24 to 29, after the Olympic Games ended, the [SO₂] started increasing a little bit. On Aug 26, the cleaning effect of the rain kept the concentration at a low level for a short time only. The whole day rain on Aug 30 reduced the [SO₂] and remained at a low level for two days. After the observation period ended, the [SO₂] began to increase slightly.

The change of [O₃] during the observation period can be roughly divided into three phases. The first phase was from Jul 28 to Aug 8. During this period, because of the rain on Jul 29 and 31, the concentration of O₃ was low. From Aug 2 to Aug 8, the [O₃] remained relatively high. On Aug 2, we observed the highest concentration, which was 128 ppbv. The second phase was from Aug 8 to Aug 23, during this period, the [O₃] was relatively low except Aug 19, which was nearly 100 ppbv. The third phase was from Aug 24 to Sep 2, the concentration exceeded 100 ppbv on Aug 24, 25 and 28. It became the second pollution period of O₃ during the observation period. After the washing effect of the heavy rain on Aug 29 and 30, the [O₃] was reduced to a relatively low level in the following days.

The changes of [NO] and [NO₂] were quite gentle. The rain had little effects on them. Contrarily, because of the weak photochemical reaction and the weak atmospheric diffusion ability in rainy days, their concentrations were actually increased such as on Aug 15 and 16. On Aug 23, we observed a high pulse peak, which might be due to the increase of traffic flow for the closing ceremony. [NO] and [NO₂] both reached the largest value, 55.8 ppbv and 52.8 ppbv. [NO₂] was remained at a very high level from Aug 2 to Aug 10, especially the concentration baseline of NO₂, it increased significantly, and reached the peak value. This was due to the steady weather which accumulated a lot of NO₂. Detailed analysis will be provided in the following section.

In addition, to focus our discussion on the formation of high-ozone, daily maximum 1-h averaged [O₃]>100 ppbv was set as the criterion to define high-ozone days. Thus there were 3 high-O₃ episodes (Aug 2, Aug 3 and Aug 24) that occurred during the observation period. The episode characteristics will be discussed in detail in the following sections.

Moreover, to focus our discussion at the formation of high-ozone events, daily maximum 1-h averaged [O₃]>100 ppbv was set as the criterion to define high-ozone days. Thus there were 2 high-O₃ episodes (August 2–3, 24–25) that occurred during the campaign. The episode features will be discussed in detail in the following sections.

3.2. Episode analysis (2008-8-2, 2008-8-3 and 2008-8-24)

On Aug 2, 3 and 24, 2008, we observed more serious photochemical pollution (as shown in Fig. 2). The maximum hourly average [O₃] reached 128 ppbv, 111.3 ppbv and 118 ppbv respectively, which was around 11%–28% higher than the China Class II standard (the mean 1-hour value is 200 $\mu\text{g m}^{-3}$ ≈ 100 ppbv based on the Environmental Air Quality Standard of China GB3095-1996, 2000 revised version). Here is the analysis of those events.

In the night of Aug 2, [NO_x] especially, the NO₂ was relatively high. From Aug 2 0500 LST, due to the solar radiation and disturbance of human activities in the urban areas, the boundary layer began to rise, and photochemical reaction started. It was a weekend day, the traffic exhaust emissions during the morning peak decreased. There was no new supplement to NO₂, and [NO₂] began to decrease through conversion and diffusion. At the same time, O₃ and NO₂ began to increase due to the photochemical reaction. [O₃] reached its first peak of 120 ppbv at 1400 LST, and then declined a bit at 1500 LST. It

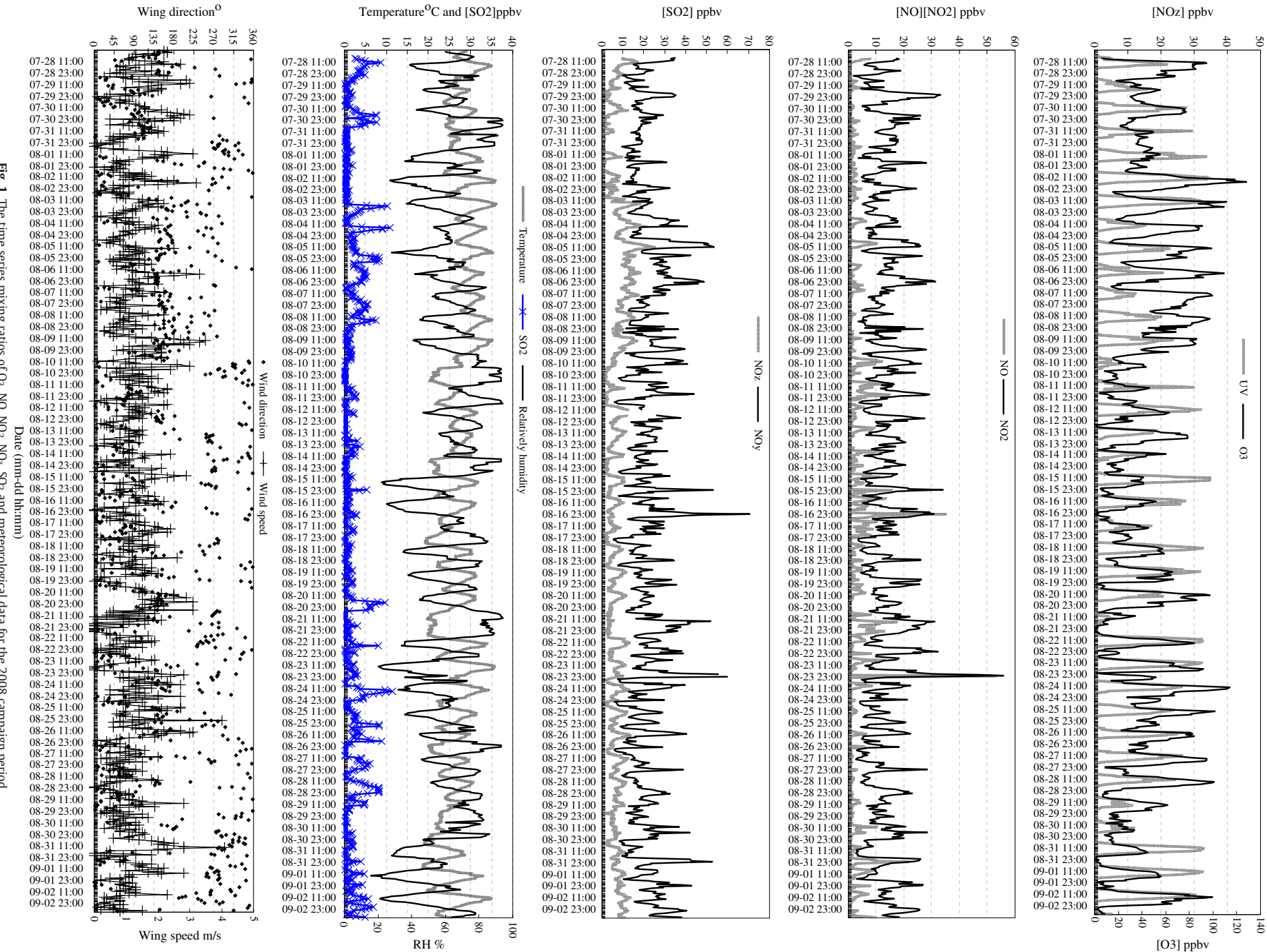


Fig. 1. The time series mixing ratios of O_3 , NO, NO₂, NO_z, SO₂ and meteorological data for the 2008 campaign period.

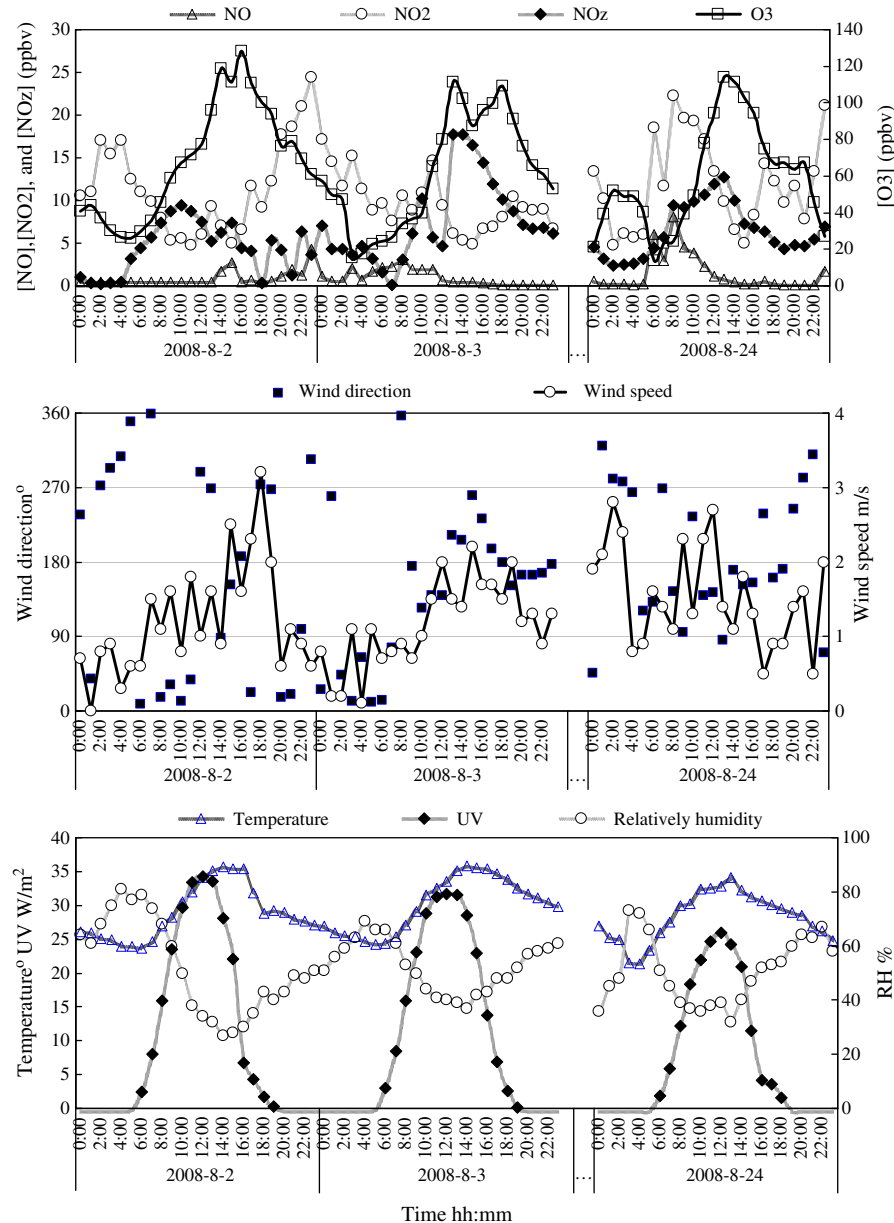


Fig. 2. Time series for the mixing ratios of NO, NO₂, NO_z, O₃, and meteorological data during August 2–3 and 24 2008.

increased again at 1600 LST and reached the maximum concentration of 128 ppbv during the entire study period then it started to decrease, the lowest value of 15 ppbv was appeared at 0300 LST on Aug 3. During the daytime of Aug 3, [O₃] was still very high, and it reached the peak value at 1300 LST. Between 1400 LST and 1500 LST, [NO] suddenly increased. This may be due to the new traffic exhaust emissions around the observation station, and it also resulted in the reducing of [O₃] to 111 ppbv by titration. However, since the input of NO was not sustaining, the photochemical reaction was still ongoing, and the wind was blown from the seriously polluted south area, [O₃] reached to the second peak value (110 ppbv) at 1800 LST because of the local superposition. Since 0000 LST of Aug 24, [O₃] started an increasing process. Meanwhile the relative humidity was also estimated to start increasing from the wind speed and wind direction data. During this period, the wind was mainly from the west, and the wind speed remained between 2 and 3 m/s for several hours. NO_y was reduced because of the decreasing of NO₂ during this period. NO_z was also reduced slowly. Since 0600 LST, the density of each pollutant and the meteorological conditions had remarkable changes. It dropped to less

than 1 ppbv at 1300 LST and this value remained during the whole night. The process of NO₂ increasing was similar to that of NO. At 0800 LST, the relative humidity was reduced greatly, and the ultraviolet radiation increased rapidly. The temperature also increased. All of these conditions led to the enhancement of photochemical reaction. During the period from 0800 to 1400 LST, it was obviously observed that NO₂ was reduced, but NO_z and O₃ increased.

Three days with high [O₃] were compared, and the max value of 128 ppbv occurred on Aug 2. The variety range of [NO_y] was not significant during the daytime. The [NO_z] increased with the increasing of [O₃] before 11:00, but the max [O₃] appeared at 16:00. The wind was in north direction before 12:00, then it turned to south direction and the wind speed increased to nearly 3 m/s (Fig. 2). The wind transported the polluting air from the south to our observation point, therefore, although the max value appeared, but the photochemistry reaction intensity was not the strongest at that time (1600 LST). The weather condition was suitable for air photochemistry reaction with high UV (34 W m⁻²), high temperatures (36 °C) and low humidity (27%) on this day.

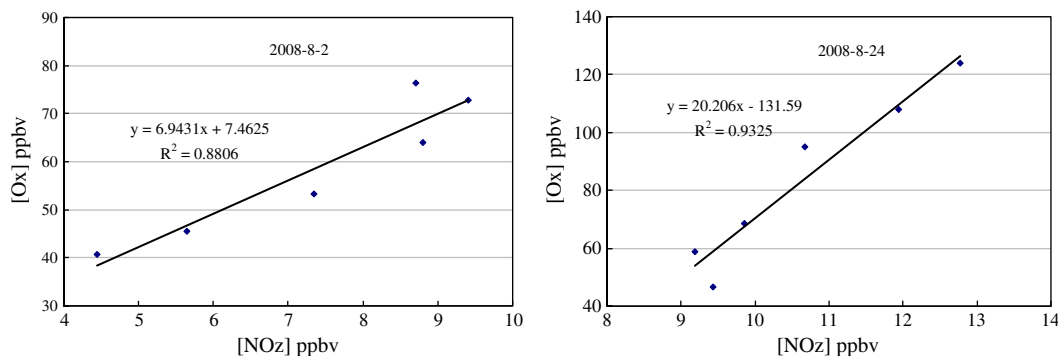


Fig. 3. OPE (NO_x) was determined from the slope of the linear regression of $[\text{O}_x]$ versus $[\text{NO}_z]$, (a) August 2 2008 and (b) August 24 2008.

The ozone concentration curve presented a double peak type on Aug 3, and the two peaks appeared at 14:00 and 18:00 respectively, which was the typical superposition effect of the local production and the regional air pollution transportation. The first peak was the local photochemistry product, but the second peak, which appeared from 1500 to 1800 with the wind direction of southwest turning to south, and the $[\text{NO}_2]$ didn't increase with the increasing of $[\text{O}_3]$, but continuously decreased. The $[\text{NO}_2]$ didn't increase with the increasing of $[\text{O}_3]$, but continuously decreased. It indicated that the air mass came from the south region at that time. The weather condition was also suitable for air photochemistry reaction with high UV (31.6 W m^{-2}), high temperatures (36°C) and low humidity (37%), and high $[\text{O}_3]$ was produced in all regions and being transmitted to the observation point when the wind direction changed.

The $[\text{O}_3]$ started fast growing since 0600 LST on Aug 24, and reached the max value at 13:00. Meanwhile, the NO_2 showed the same trend. The $[\text{NO}_y]$ was of the highest value on this day, but it had the lowest UV (26 W m^{-2}), the lowest air temperature (34°C), and the highest relative humidity (36%) in the three episodes. The wind velocity continuously increased from 6:00 to 13:00, and the wind direction still changed from north to south. This was because of the mountain-valley breeze effect. In this episode, due to the weather condition and precursor of ozone, the $[\text{O}_3]$ had the lowest value, and it was distributed uniformly.

3.3. Ozone production efficiency

Ozone production efficiency (OPE) refers to the quantity of O_3 molecules generated by removing one NO_x molecule during the atmospheric photochemical reaction (Liu et al., 1987). NO_x plays the role of catalytic and circulating in atmospheric photochemistry of O_3 , but the NO_2 in NO_x will be oxidized to HNO_3 by OH and will be removed from the atmosphere through deposition.

Therefore, the concept of OPE (NO_x) is a good indicator to assess the sensitivity to NO_x or VOCs that generate O_3 . It can also be used to calculate the amount of O_3 generated, and it can serve as the theoretical basis for the control strategy of O_3 . In addition, OPE (NO_x) can be obtained by model calculation, and it can also be calculated from the observation data, therefore, it is a good indicator for verifying model simulation results (Charles et al., 2009). Analysis of OPE (NO_x) can be directly measured by O_3 , NO_x , and NO_y , and thus the formula establishes a viable method based on the observations for calculating the ozone sensitivity to NO_x . There are many forms to express OPE (NO_x). Since photolysis of NO_2 during the day produces O_3 quickly, experimental results show that there is a significant linear correlation between O_3 and NO_y , and between O_3 and NO_2 . OPE (NO_x) is defined as: $\text{OPE}(\text{NO}_x)x = \Delta(\text{O}_3 + \text{NO}_2)/\Delta(\text{NO}_y - \text{NO}_x) = \Delta(\text{O}_x)/\Delta(\text{NO}_2)$ after improvement (Nunnermacker et al., 1998; Trainer et al., 1993).

According to the observations and simulations conducted by the scientists in different areas in recent years, it is noted that the range of

the reported OPE (NO_x) values is quite large. The values are from less than 10 in the polluted areas (Berkowitz et al., 2004; Stehr et al., 2000) to more than 100 in the clean areas (Davis et al., 1996). The variation is due to the differences of VOCs, NO_x , atmospheric oxidation, temperature, radiation, and other meteorological factors in the atmosphere of different regions. At the same time, the significant variation of OPE (NO_x) in different areas also shows that in the process of transporting the polluted air masses, as the air mass aging photochemically, NO_x is continuously oxidized and removed from the system, and the VOC control is gradually shifted toward NO_x control, which generates O_3 in the air mass in polluted areas. However, OPE (NO_x) maintains a growing trend, so $[\text{O}_3]$ rapidly increases in the smoke plume of the city, which results in the high $[\text{O}_3]$ pollution which usually occurs in the large area of dozens of kilometers leeward of the city.

It is generally believed that the further oxidation of NO_x will produce NO_2 , and $[\text{NO}_2]$ should increase with the production process of O_3 . The OPE (NO_x) for each day can be calculated from the relationship of growth between $[\text{NO}_z]$ and $[\text{O}_x]$ ($\text{O}_x = \text{O}_3 + \text{NO}_2$) during the daytime. In this paper, the O_3 production efficiency of NO_x was decided by the relationship between $[\text{O}_x]$ and $[\text{NO}_z]$ from 0800 to 1400 LST. Take the high-ozone pollution case on Aug 2 and 24 as an example. Fig. 3a and b shows the scatter diagrams that indicate the relevant changes of $[\text{O}_x]$ and $[\text{NO}_z]$ on these two days respectively. Obviously, $[\text{NO}_z]$ and $[\text{O}_x]$ have a consistent positive correlation. The data shows that OPEs (NO_x) of high O_3 pollution for these two days were 6.9 and 20.2 respectively. The OPEs (NO_x) of 6.9 on Aug 2 indicates that the pollution type was of typical city emission characteristic, and the production of O_3 came from the local sources. On the other hand, OPE (NO_x) of 20.2 on Aug 24, the day of the Olympic Games closing ceremony was larger than that of the source region of the city but lower than that of the clean area. The sensitivity of O_3 generated was transiting from VOCs control to NO_x control, which is comparable to the results of other studies (Roussel et al., 1996; Li et al., 1997). Using this slope calculation method, the OPE (NO_x) was obtained for each day from 0800 to 1400 LST during the observation period, and the average value of the maximum $[\text{O}_3]$ in each hour was extracted. There is no direct correlation between them. This is because O_3 can reach its largest concentration not only by production efficiency, but also by the non-linear relationship with the concentration of its precursors. Under the same conditions, the higher initial $[\text{NO}_x]$ and higher consumption of reaction cycle will lead to lower OPE (NO_x), therefore, OPE (NO_x) can be considered as a feature of conversion from NO_x restriction to NO_x saturation.

The guiding value proposed by Sillman (1995) is: $[\text{O}_3]/[\text{NO}_2] < 7$, which is an indicator of VOCs constraining O_3 on chemistry. In this study, the variation of OPE (NO_x) was from 4 to 22 in high O_3 days, which indicated that O_3 production was affected by both the local emission and the transportation of polluted air masses, and the O_3 production is a transitional state and tends to NO_x control in this region.

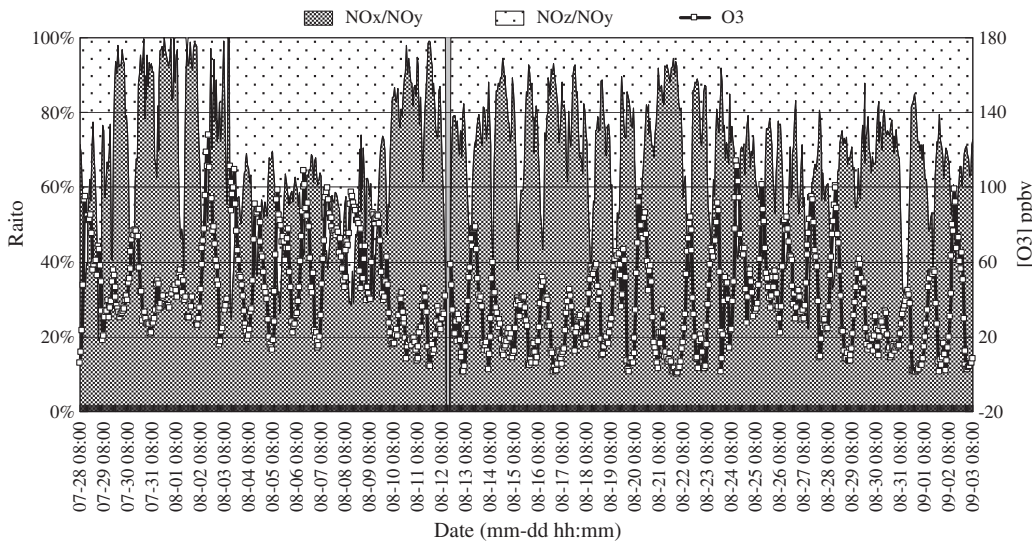


Fig. 4. Time series of $[O_3]$ compared to the partition of NO_y (NO_x and NO_z) during Aug 2 2008 to Sep 3 2008.

3.4. Others photochemical indicators (NO_x/NO_y , NO_z/NO_y , and O_3/NO_x)

For the O_3 control strategy research, besides numerical models and the Empirical Kinetic Modeling Approach (EKMA) curve method, photochemical indicator discrimination based on observations has also been widely used. The principle is to evaluate the sensitivity of O_3 generation and to observe the chemical properties of air masses by considering the ratio of the concentration changes between O_3 itself and its precursors as the indicator, such as O_3/NO_y , O_x/NO_y , NO_z/NO_y , $H_2O_2/(NO_y-NO_x)$ and $HCHO/NO_y$, etc. (Sillman, 1995).

As Fig. 4 shows, the low NO_z/NO_y and high NO_x/NO_y occurred almost every morning before 0800 LST. This means that at this period the atmosphere was in the state of pollutant input, which is due to the superposition effects of the local traffic emissions, the convective flow in mixed layers, and the NO_2 night elimination settling. From 0800 LST to noon, the NO_z/NO_y ratio increased while the NO_x/NO_y ratio decreased. During this period, $[O_3]$ also increased rapidly. On Aug 3 and Aug 9, the ratio of NO_z/NO_y was still very high, without obvious diurnal variation. According to the meteorological data, the temperature remained at a high level during this period. The daily average temperature from Aug 3 to Aug 9 was 30 °C, which the average temperature for the entire August was 26 °C. The relative humidity was relatively low, around 59%, and the average value during the entire observation was 62%. The wind direction was mainly SSW. Under such kind of meteorological conditions, the local emitted fresh pollutants could not be easily spread, and the old air mass remained to come from the south, so the photochemical reaction product could not easily proliferate, and caused $[NO_z]$ and $[O_3]$ to remain at a high level. Therefore, the relevant indicators developed from the

concentration of NO_y and NO_z and the ratios of NO_x/NO_y and NO_z/NO_y can be used to analyze the simulation results to explore the role and impact of O_3 photochemical pollution in the transportation process.

The interactions $\Delta(O_3)/\Delta(NO_x)$ as a characterization of O_3 generation and the elimination of NO_x from the system show that NO_2 in the NO_x pool will cycle in the photochemical reactions, and at the same time react with VOCs free radicals to generate NO_z and be eliminated from the system.

Through the correlation analysis by making a scatter diagram of $[O_3]$ and $[NO_x]$ data in the photochemical reaction developing process from the two episodes of high $[O_3]$ from 0900 to 1300 LST on Aug 2 and Aug 24, a linear relationship was obtained as shown in Fig. 5. The $[O_3]$ and $[NO_x]$ data showed a very strong inverse correlation. R^2 reached 0.95 and 0.97 respectively, and the slope was -0.171 and -0.2 respectively. On Aug 2, although the maximum hourly average value of $[O_3]$ was higher than that on Aug 24, from Fig. 5, with the production of O_3 , the NO_x decreased more rapidly than it did on Aug 24. Referring to Section 3.3, the OPE (NO_x) value on 24 was higher, which indicated that on this day, NO_x produced O_3 more effectively. This meant that less NO_x would produce more O_3 . Fig. 5 actually indicated that NO_x was less on the 2nd, but it produced more $[O_3]$ eventually. In fact, this was not contradictory. According to the OPE (NO_x) analysis, the background of NO_x on the 24th was high, and the wind direction frequency mostly came from south and belonged to the previous air mass. However, the background of NO_x on the 2nd was low, and the wind direction frequency mostly came from north and belonged to the fresh air mass. Therefore, the pollution of high concentration of O_3 on Aug 2 was due to the local source premise

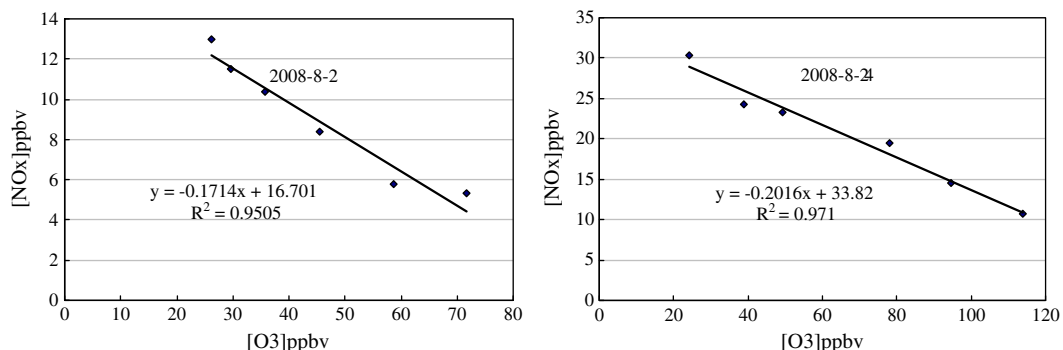


Fig. 5. Correlation analysis of $[O_3]$ and $[NO_x]$: (a) Aug 2 2008 and (b) Aug 24 2008.

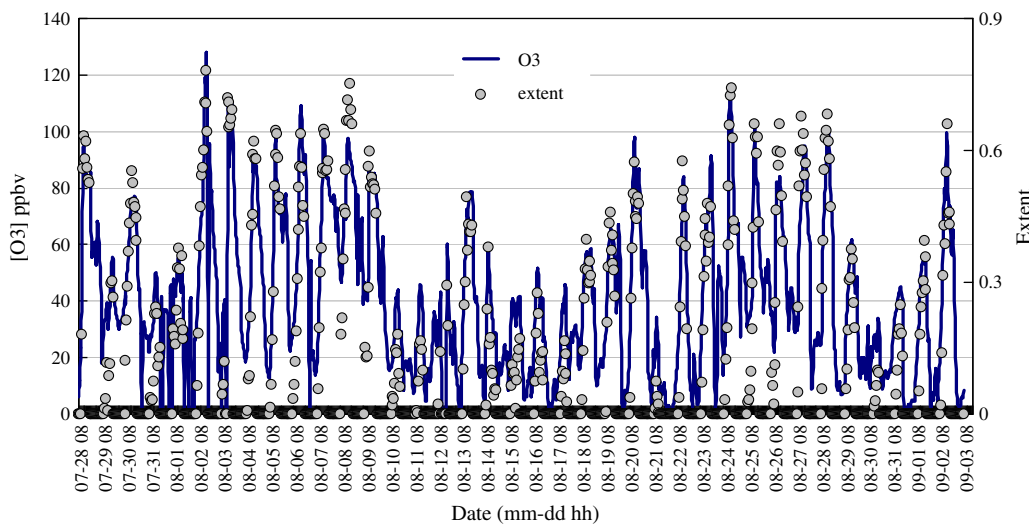


Fig. 6. Time series of $[O_3]$ and extent during the 2008 campaign period.

photochemical reaction, while that of Aug 24 was due to the superimposition of peripheral air mass transmission pollution and the local photochemical pollution.

3.5. Smog production model

The Smog Production Model (SPM) is a type of semi-empirical formula which is based on O₃ and NO_x to observe the degree of photochemical reaction and decide which restricts O₃ more, between VOCs or NO_x. It was firstly studied by the Graham Johnson team in Australia in (1984), and then [Blanchard et al. \(1999\)](#) and [Chang et al. \(1997\)](#) observed smog chamber data to amend the basic assumption parameters in the SP algorithm to improve the accuracy for forecasting ozone sensitivity (VOCs or NO_x control). In this study, the SPM is applied to assess the sensitivity of O₃ qualitatively in the region and the effect of the relative trends between VOCs and NO_x control. The explanations for the SPM results are that, when reaction extent is less than 0.6, it represents strong VOCs constrain; when reaction extent is between 0.6 and 0.9, it represents the transition to NO_x control, and when the reaction extent is more than 0.9, it represents strong NO_x control. In previous studies, the NO_x environmental monitoring by standard equipment (to measure NO₂ by the molybdenum conversion method) generated great errors by the inclusion of HNO₃, PAN, and some NO_x in the measurement. These measurements were neither true NO_x, nor true NO_y. While in this study, the NO₂ was measured by light conversion to obtain precise NO_x concentrations, and thus the results were more accurate. The decisions about control over ozone production will be obtained with this method.

Through the calculation of average value of O₃, NO, and NO₂ per hour during the daytime, time series of these parameters related to reaction level and [O₃] were obtained together (as Fig. 6). According to the figure, there are 24 days in the observation period with the extent value smaller than 0.6, and 14 days with the value larger than 0.6. However, there are no days with the extent value larger than 0.8, which indicated that the observation station was not a NO_x sensitive system during the observation period. When high [O₃] occurred on Aug 2 and Aug 24, the extent value of the maximum O₃ was 0.78 and 0.74 respectively. This belonged to the transition state when VOCs sensitiveness transmitted to the NO_x sensitiveness, which was consistent with the analysis result of OPE (NO_x) in Section 3.4. It also showed that the high concentration of O₃ at the observation point was due to the compound influences of urban sources themselves and the peripheral transmission of air mass.

Analysis of the extent of reaction, the wind data and their association (as Fig. 7), shows that when extent of reaction is greater than 0.6, the wind direction is basically from the southeast. The reaction time of the air mass from this direction is relatively long, and its photochemical age is relatively old. This is due to the windward influence on photochemical pollution at the observation station in summer.

4. Conclusions

There was strict emission control during the Beijing Olympic Games in 2008, and many pollutants were at a lower level. However, [O₃], which is one of the most difficult air quality problems in the world, was still high in August.

On Aug 2, 3 and 24 2008, the more serious photochemical pollution was observed at the observation station. The largest hourly average of [O₃] reached 128.2 ppbv, about 28% higher than China Class II standard (the mean 1-hour value is 200 $\mu\text{g m}^{-3} \approx 100$ ppbv, from the Environmental Air Quality Standard of China GB3095-1996, 2000 revised version). The data showed a pollution episode caused by superposition of local photochemical reactions and the regional

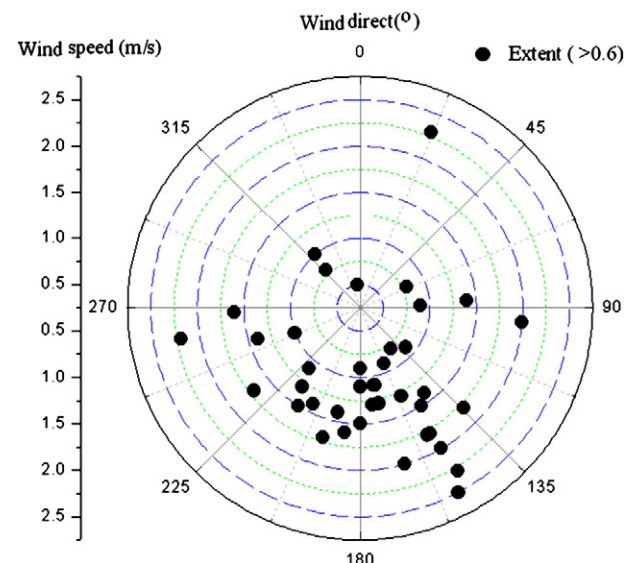


Fig. 7. Analysis of extent of reaction and wind data (when extent of reaction >0.6).

transportation. The observation showed that the OPEs (NO_x) of high O_3 pollution during the observation period were 6.9 and 20.2 ppbv, and there was an obvious change. The OPE (NO_x) of 6.9 on Aug 2 belonged to a typical city source area characteristic, it implied that the high O_3 could be due to the local sources. The OPE (NO_x) of 20.2 on Aug 24, the Olympics Closing Ceremony day was larger than the source region in the city but lower than that of the surrounding clean area. It suggested that the pollution is because of regional transferring.

60% of the extent data was less than 0.6 and the rest was slightly larger than 0.6, with maximum of 0.78. This indicated that the sensitivity of O_3 generated was VOCs control during the observation period. The SPM results also implied that the high- O_3 is in a transition state from VOCs sensitivity to NO_x sensitivity. It showed that the photochemical pollution at the observation station was mostly subject to the influence of southeast air flow in the summer.

Acknowledgments

I would like to thank Senior Engineer Liu Guangren for providing a great deal of assistance in the completion of the experiments. The work presented in this paper was supported by the National Key Basic Research and Development Plan (973 project) (2007CB407303), the grant of the Knowledge Innovation Program of Chinese Academy of Sciences (approved # KZCX1-YW-06-01) and the Hi-tech Research and Development Program of China (Grant No. 2006AA06A301). Project of Evaluation and Forecast Air Quality During the Beijing 2008 Olympic Games from the Beijing Municipal Environmental Protection Bureau and the Public Project of Beijing Municipal Science & Technology Commission (D09040903670902).

References

- Ariel FS, Mantilla E, Millán M. Using measured and modeled indicators to assess ozone- NO_x -VOCs sensitivity in a western Mediterranean coastal environment. *Atmos Environ* 2005;39:7167–80.
- Berkowitz CM, Jobson T, Jiang G, Spicer CW, Doskey PV. Chemical and meteorological characteristics associated with rapid increases of O_3 in Houston, Texas. *J Geophys Res* 2004;109(D10307). doi:10.1029/2003JD004141.
- Blanchard CL, Lurmann FW, Roth PM, Jeffries HE, Korc M. The use of ambient data to corroborate analyses of ozone control strategies. *Atmospheric Environment* 1999;33(3):369–81.
- Cardelino CA, Chameides WL. Natural hydrocarbon, urbanization, and urban ozone. *J Geophys Res* 1990;95(D9):13971–9.
- Carl M, Berkowitz RA, Bian ZX, Zhong S, Robert S, Disselkamp NS, Laulainen EGC. Aircraft observations of aerosols, O_3 and NO_y in a nighttime urban plume. *Atmos Environ* 2001;35:2395–404.
- Cassandra VH, Munger JW, Steven CW, Zahniser M, Nelson DJ, McManus B. Atmospheric reactive nitrogen concentration and flux budgets at a Northeastern U.S. forest site. *Agric For Meteorol* 2006;136:159–74.
- Chameides WL, Lindsay RW, Richardson J, Kiang CS. The role of biogenic hydrocarbons in urban photochemical smog: Atlanta as case study. *Science* 1988;241:1473.
- Chang TY, Chock DP, Nance BI, Winkler SL. A photochemical extent parameter to aid ozone air quality management. *Atmos Environ*. 1997;2787–94.
- Charles CK, Chou CYT, Chein JS, Liu SC, Zhu T. Measurement of NO_y during campaign of air quality research in Beijing 2006 (CAREBeijing-2006): implications for the ozone production efficiency of NO_x . *J Geophys Res* 2009;114:D00G01, doi:10.1029/2008JD010446.
- Davis DD, Crawford J, Chen G, Chameides W, Liu S, Bradshaw J, et al. Assessment of ozone photochemistry in western North Pacific as inferred from PEM-West A observations during fall 1991. *J Geophys Res* 1996;101(D1):2111–34.
- Guangfeng J, Jerome DF. Modeling the effects of VOCs and NOX emission sources on ozone formation in Houston during the TexAQS 2000 field campaign. *Atmos Environ* 2004;38:5071–85.
- Li SM, Anlauf KG, Wiebe HA, Bottenheim JW, Shepson PB, Biesenthal T. Emission ratios and photochemical production efficiencies of nitrogen oxides, ketones, and aldehydes in the lower Fraser Valley during the Summer Pacific 1993 Oxidant Study. *Atmos Environ* 1997;31:2037–48.
- Liu SC, Trainer M, Fehnisenfeld FC, Parrish DD, Williams Ej, Fahey DW, et al. Ozone production in the rural troposphere and the implications for regional and global ozone distributions. *J Geophys Res* 1987;92(D4):4191–207.
- Mannschreck K, Gilge S, Duelmer PC, Fricke W, Berresheim H. Assessment of the applicability of $\text{NO}-\text{NO}_2-\text{O}_3$ photostationary state to long-term measurements at the Hohenpeissenberg GAW Station, Germany. *Atmos Chem Phys* 2004;4:1265–77.
- Nunnermacker IJ, Imre D, Daum PH, Kleinman L, Lee Y-N, Lee JH, Springston SR, et al. Characterization of the Nashville urban plume on July 3 and July 18, 1995. *J Geophys Res* 1998;103:28129–48.
- Paul O, Wennberg Donald D. Rethinking ozone production. *Science* 2008;319 March 21.
- Penga YP, Chena KS, Laib CH, Lua PJ, Kaoa JH. Concentrations of H_2O_2 and HNO_3 and O_3 -VOCs- NO_x sensitivity in ambient air in southern Taiwan. *Atmos Environ* 2006;40:6741–51.
- Rai vonen M, Vesala T, Pirjola L, Altimir N, Keronen P, Kulmala M, Hari P. Compensation point of NO_x exchange: net result of NO_x consumption and production. *Agric For Meteorol* 2009;49:1073–81.
- Roussel PB, Lin X, Camacho F, Laszlo S, Taylor R, Melo OT, et al. Observations of ozone and precursors at two sites around Toronto, Ontario, during SONTOS 92. *Atmos Environ* 1996;30:2145–55.
- Sillman S. The use of NO_y , H_2O_2 and HNO_3 as indicators for ozone- NO_x -hydrocarbon sensitivity in urban locations. *J Geophys Res* 1995;100:14175–88.
- Stehr JW, Dickerson RR, Hallock-Waters KA, Doddridge BG, Kirk D. Observations of NO_y , CO , and SO_2 and the origin of reactive nitrogen in the eastern United States. *J Geophys Res* 2000;105:3553.
- Thomas AV, Berg M, Heil T, Houben AN, Lerner W, Petrick DR, Pätz HW. Measurements of total odd nitrogen (NO_y) aboard MOZAIC in-service aircraft: instrument design, operation and performance. *Atmos Chem Phys* 2005;5:583–95.
- Trainer M, Parrish DD, Buhr MP, Norton RB, Fehnisenfeld FC, Anlauf KG. Correlation of ozone with NO_y in photochemically aged air. *J Geophys Res* 1993;98:2917–85.
- Wang Y, Hao J, McElroy MB, Munger JW, Ma H, Chen D, Nielsen CP. Ozone air quality during the 2008 Beijing Olympics: effectiveness of emission restrictions. *Atmos Chem Phys* 2009;9:5237–51.
- Wang T, Nie W, Gao J, Xue LK, Gao XM, Wang XF, Qiu J, Poon CN, Meinardi S, Blake D, Ding Aj, Chai FH, Zhang QZ, Wang WX. Air quality during the 2008 Beijing Olympics: secondary pollutants and regional impact. *Atmos Chem Phys Discuss* 2010;10:12433–63.
- Zhang L, Wiebe A, Vet R, Mihele C, Jason M, Brien O, Iqbal S, Liang Z. Measurements of reactive oxidized nitrogen at eight Canadian rural sites. *Atmos Environ* 2008;42:8065–78.